

## The Vela Pulsar Progenitor Was Most Likely a Binary Merger

JEREMIAH W. MURPHY <sup>1</sup>, ANDRÉS F. BARRIENTOS,<sup>2</sup> RENÉ ANDRAE <sup>3</sup>, JOSEPH GUZMAN,<sup>1</sup> BENJAMIN F. WILLIAMS <sup>4</sup>,  
JULIANNE J. DALCANTON <sup>5</sup> AND BRAD KOPLITZ <sup>6</sup>

<sup>1</sup>*Department of Physics  
Florida State University  
77 Chieftan Way  
Tallahassee, 32306, FL, USA*

<sup>2</sup>*Department of Statistics  
Florida State University  
117 N. Woodward Ave.  
Tallahassee, 32306, FL, USA*

<sup>3</sup>*Max-Planck-Institut für Astronomie  
Königstuhl 17  
Heidelberg, D-69117, Germany*

<sup>4</sup>*Department of Astronomy  
University of Washington  
Box 351580  
Seattle, WA, 98195, USA*

<sup>5</sup>*Center for Computational Astrophysics  
Flatiron Institute  
162 Fifth Ave New York, NY, 10010, USA*

<sup>6</sup>*School of Earth & Space Exploration  
Arizona State University  
781 Terrace Mall  
Tempe, AZ, 85287, USA*

### ABSTRACT

Stellar evolution theory restricted to single stars predicts a minimum mass for core-collapse supernovae (CCSNe) of around eight solar masses; this minimum mass corresponds to a maximum age of around 45 million years for the progenitor and the coeval population of stars. Binary evolution complicates this prediction. For example, an older stellar population around 100 million years could contain stellar mergers that reach the minimum mass for core collapse. Despite this clear prediction by binary evolution, there are few, if any CCSNe associated with a distinctly older stellar population...until now. The stellar population within 150 pc of the Vela Pulsar is inconsistent with single-star evolution only; instead, the most likely solution is that the stellar population is  $\geq 80$  Myr old, and the brightest stars are mass gainers and/or mergers, the result of binary evolution. The evidence is as follows. Even though the main sequence is clearly dominated by a  $\geq 80$ -Myr-old population, a large fraction of the corresponding red giants is missing. The best-fitting single-star model expects 51.5 red giants, yet there are only 22; the Poisson probability of this is  $1.7 \times 10^{-6}$ . In addition, there is an overabundance of bright, young-looking stars (25-30 Myrs old), yet there is not a corresponding young main sequence (MS). Upon closer inspection, the vast majority of the young-looking stars show either past or current signs of binary evolution. These new results are possible due to exquisite Gaia parallaxes and a new age-dating software called *Stellar Ages*.

*Keywords:* Core-collapse supernovae (304) — Pulsars (1306) — Stellar associations (1582) — Multiple star evolution (2153)

## 1. INTRODUCTION

The association of the Vela Pulsar with the Vela Supernova Remnant (SNR) was one of the first observations to support the hypothesis that core-collapse supernovae (CCSNe) indeed produce neutron stars (Large et al. 1968). The next obvious question is what was the progenitor that produced both the Vela SNR and the Vela Pulsar. While the progenitor likely exploded relatively recently ( $\sim 20,000$  yrs ago) (Dodson et al. 2003), this was well before reliable stellar records, so there are no records of the progenitor. Another way to characterize the progenitor is to age-date the stellar population near the SNR, and from this age, infer the progenitor mass (Badenes et al. 2009; Jennings et al. 2014; Williams et al. 2018; Díaz-Rodríguez et al. 2018; Koplitz et al. 2021). But this requires reliably identifying all stars near the Vela Pulsar. Until recently, the Vela Pulsar was both too far and too close to reliably age-date the surrounding stellar population. While the Hipparcos Catalog provides distances to the nearest stars, it can not provide a complete picture at the distance of the Vela Pulsar,  $287_{-17}^{+19}$  pc (Dodson et al. 2003). Ironically, it is easier to identify stellar populations outside of our galaxy, where the relative distances between the stars is much smaller than the distance to the external galaxy. Gaia has made it possible to identify stellar populations within our galaxy, enabling age-dating techniques that were relegated to nearby galaxies. Using Gaia parallaxes supplemented by Hipparcos parallaxes for the brightest stars, Kochanek (2022) age-dated the stellar population near the Vela Pulsar and inferred a progenitor mass of 8.1-10.3  $M_{\odot}$ ; it is crucially important to note that the Kochanek (2022) analysis assumed single-star evolution. In this manuscript, we re-analyze the stellar population age using a new age-dating algorithm (*Stellar Ages*). This analysis indicates that the stellar population is inconsistent with single-star evolution only and the most likely scenario is that the Vela Pulsar progenitor was a merger or mass-gainer.

Stellar evolution theory predicts that massive stars with masses  $\gtrsim 8 M_{\odot}$  undergo core collapse (Woosley et al. 2002). What is less clear is which stars subsequently explode, leaving behind a NS and which collapse to a black hole, aborting the explosion. Coarsely, there are three approaches to theoretically predicting which stars explode. One is to simulate CCSNe using expensive multidimensional radiation-hydrodynamic simulations (Lentz et al. 2015; Bruenn et al. 2016; Müller

2015, 2016; Vartanyan et al. 2018; Burrows & Vartanyan 2021). A second approach is to force one-dimensional simulations to explode by calibrating them against observations or multi-D simulations (Sukhbold et al. 2016; Mabanta et al. 2019; Couch et al. 2020; Ghosh et al. 2021). The third approach is to develop analytic explosion conditions (Burrows & Goshy 1993; Pejcha & Thompson 2012; Murphy & Dolence 2017; Gogilashvili & Murphy 2022). In any case, our understanding of which stars explode is only as good as our observational constraints of which stars actually explode.

There are three broad strategies to characterize the progenitors of CCSNe. One is to model the supernova brightness evolution, and infer the total ejecta mass or the size of the Fe core that exploded (Bartunov et al. 1994; Moriya et al. 2011; Kasen & Woosley 2009; Hillier & Dessart 2012; Morozova et al. 2015; Barker et al. 2023). A second is to use serendipitous pre-imaging to model the brightness and color of the progenitor (Smartt 2015; Van Dyk 2017; Strotjohann et al. 2023). From these observations, one infers the mass of the star that exploded. The third is to age-date the surrounding stellar population, and from this age infer the zero-age main sequence (ZAMS) mass of the star that exploded (Gogarten et al. 2009; Williams et al. 2018; Koplitz et al. 2023; Díaz-Rodríguez et al. 2021). The general principle of the age-dating technique is to model the brightnesses and colors (color-magnitude diagram: CMD) of not just one star, but all of the stars within about  $\sim 100$  pc of SN location. In modeling the CMD, one infers the age (or multiple ages) that reproduces the observed stellar population. Since the progenitor of the Vela SNR and Pulsar exploded more than 10,000 years ago, we must use the third option: age-dating the surrounding stellar population.

The age-dating technique has been used to infer the progenitor masses for hundreds of CCSNe. In particular, when SN and progenitor observations do not exist, then the age-dating technique provides the only means for progenitor mass estimates. For example, Williams et al. (2018) inferred the progenitor masses for all historic SNe within about 8 Mpc. Jennings et al. (2014) inferred the ages and progenitor masses for 115 SNRs, and using this sample, Díaz-Rodríguez et al. (2018) inferred the progenitor mass distribution. In fact, they find a minimum mass for CCSN of  $7.3 \pm 0.1 M_{\odot}$  and this minimum mass remains the most precise statistical inference to date.

Age-dating also provides one of the few means to inferring progenitor properties for compact remnants such as neutron stars. The Vela Pulsar is a prime candidate; it is quite young, still embedded within its coeval stellar population, is relatively close ( $\sim 300$  pc), and has a precise distance. Kochanek (2022) used the age-dating technique to infer a most likely age and mass for the Vela Pulsar Progenitor. Like all age-dating analyses before, that analysis used Poisson statistics to model the number of stars in the CMD. This analysis also used single-star stellar evolution models to model the brightness and colors of the theoretical CMD. Again, this is standard practice. For the data, Kochanek (2022) used Gaia magnitudes and parallaxes. To account for completeness, they also included 9 bright stars that are in the Hipparcos catalog but not in the Gaia catalog. In the mixture model, Kochanek (2022) found a range of ages older than  $\log_{10}(t/\text{yr}) = 7.4$  that reproduces the observed CMD. Associating the progenitor with the youngest age,  $10^{7.4} - 10^{7.6}$  years, they suggest that the progenitor ZAMS mass was  $8.1\text{-}10.3 M_{\odot}$ .

In spite of the demonstrated promise of age-dating, most existing studies including that of Kochanek (2022), have relied predominantly on single-star evolution models. This reliance on single-star evolutionary models is true despite clear observations and predictions that binary evolution can significantly alter the magnitude and colors of the progenitors. Spectroscopic observations of massive stars shows that 70% of massive stars are in binaries (Sana et al. 2012), and binary evolution suggests that around 30% of these systems will have their evolution affected by mass transfer, and 8% of massive star systems may in fact merge. Recently, Menon et al. (2024) show that binary evolution significantly alters the fraction of blue supergiants in a stellar population; hence, binary evolution directly impacts the brightness and colors of the associated stellar population. Zapartas et al. (2017) showed that roughly 15% of CCSNe should be associated with relatively old stellar populations. Single-star evolution predicts that the maximum age for the surrounding stellar population would be about  $\sim 45$  Myr. However, the merger of two  $4 M_{\odot}$  stars near the end of their lives ( $\sim 100$  Myr) could result in a rejuvenated star that explodes. Hence, binary evolution naturally predicts that some CCSNe should be associated with older stellar populations. Yet, a clear association with an older ( $\sim 100$  Myr old) population has remained elusive.

If binary evolution is expected to impact massive star evolution, brightnesses and colors, why have all age-dating methods used single-star evolution? For one, in all previous analyses, the theoretical CMDs fit the data

reasonably well and typically revealed a population with an age  $< 50$  Myr. Also, because the SN type that produced the SNR is typically not known, if no young population is found, it is possible that the event was not a core-collapse SN (such as a Type Ia). Furthermore, modeling CMDs that include binary evolution would require significantly more work...and parameters. In the spirit of Occam’s Razor, why over complicate the CMD models if the data does not demand it?

As the subsequent sections show, a new, more discerning age-dating algorithm shows that the stellar population surrounding the Vela Pulsar is clearly inconsistent with a CMD generated by single-star models only. The primary reason for this inconsistency while all previous analyses were consistent is a change in the likelihood model. In all previous analyses, the Likelihood modeled the number of stars with Poisson statistics. However, modeling the number of the brightest and rarest stars on the CMD is highly susceptible to low-number statistics. Unfortunately, these statistical models were not discerning enough to rule out the single-star models when inferring the ages of stellar populations.

Rather than modeling the observed number of stars, the statistical model of this manuscript uses joint probability density functions to model the age for each star. This shift in statistical approach more effectively maximizes the age information of a stellar population that includes young, bright, and rare stars. It is also this shift in statistical approach that illuminates the clear inconsistency of the Vela Pulsar stellar population with single-star only models.

The following manuscript presents the case as follows. Section 2 describes the selection of the stellar population within 150 pc of the Vela Pulsar. This is only possible because of Gaia parallaxes. However, for these bright stars, Gaia is incomplete, so we supplement missing stars with the Hipparcos catalog. Section 3 describes the statistical model and Bayesian inference for the mixture of ages and metallicities. Section 4 presents the results and shows how the data is inconsistent with this inference which relies on single-star models. Section 5 presents a cross correlation of the brightest stars with identified stars within the Simbad Database and discusses how these identifications further support that the brightest stars are likely the product of binary evolution. Finally, we summarize the main assumptions and results in section 6.

## 2. DATA SELECTION, CORRECTION, AND VERIFICATION

Age-dating the stellar population near the Vela Pulsar is possible because of exquisite parallaxes of the Vela

Pulsar (from VLBI) and the surrounding stars (from Gaia).

The location and space motion of the Vela Pulsar have been well-measured some two decades ago, when [Dodson et al. \(2003\)](#) provided an accurate astrometric solution from VLBI observations, including sky coordinates, parallax, and proper motion. On the sky, the pulsar is located to a tiny fraction of an arcsecond ( $\alpha = 08^{\text{h}}35^{\text{m}}20.61149^{\text{s}} \pm 0.00002^{\text{s}}$  and  $\delta = -45^{\circ}10'34.8751'' \pm 0.0003$  in the 2000.0 epoch). This corresponds to galactic coordinates of  $(l, b) = (263.55183143^{\circ}, -2.78731237^{\circ})$ . The pulsar is also quite close, with a parallax of  $3.5 \pm 0.2$  mas, which corresponds to  $287_{-17}^{+19}$  pc. Given these coordinates and distance, the Vela Pulsar is  $\sim 14$  pc below the galactic plane, which puts it squarely within the Milky Way’s thin disk.

[Dodson et al. \(2003\)](#) infer a transverse space velocity of  $61 \pm 2$  km s $^{-1}$  with respect to local standard of rest. This is a somewhat pedestrian space velocity for a pulsar ([Hansen & Phinney 1997](#)), increasing the likelihood that the pulsar is still embedded within its parent stellar population. Combining this proper motion with the distance to the center of Vela supernova remnant (SNR) of  $25 \pm 5$  arcmin ([Aschenbach et al. 1995](#)), [Kochanek \(2022\)](#) estimates an age of  $\sim 20,000$  yrs for the pulsar. The corresponding physical distance traveled during this young age is only  $\sim 1.5$  pc. All of this evidence strongly suggests that the Vela Pulsar is still embedded within its birth coeval stellar population.

We identify this local stellar population using Gaia Data Release 3 (DR3) ([Gaia Collaboration et al. 2016, 2022](#)). We use the following search criteria to select all stars with good quality data within 150 pc of the Vela Pulsar: 1) Sky coordinates within 27 degrees of the Vela Pulsar position; 2) parallaxes between 2.2727 and 7.1429 mas; and 3) a bp apparent magnitude less than 10. This last constraint reduces the size of the stellar population to model by providing a first rough cut in magnitude. Given the distances, this roughly corresponds to an absolute magnitude of 2. The absolute magnitudes in RP are

$$M_{RP} = G_{RP} - 5 \log_{10} \left( \frac{1000}{10(\varpi - z_{\text{pt}})} \right) - A_{RP} \quad (1)$$

where  $G_{RP}$  is the Gaia apparent magnitude,  $\varpi$  is the parallax in milliarcseconds,  $z_{\text{pt}}$  is the zero point ([Lindgren et al. 2021](#)), and  $A_{RP}$  is the GSP-Phot extinction. We similarly calculate the absolute magnitudes in BP. After calculating these absolute magnitudes, we further restrict the stellar population to absolute magnitudes brighter than 0 in both BP and RP. These lower bounds on brightness roughly correspond to the brightness of a  $3-M_{\odot}$  main sequence (MS) star.

Extinction can significantly affect the color and magnitude of stars. Even though the stars surrounding the Vela Pulsar are relatively close, it is important to measure the extinction and correct the absolute magnitudes where necessary. There are typically two strategies to account for extinction. One strategy is to include the variance in modeling the CMDs. [Kochanek \(2022\)](#) adopted this strategy when inferring the ages of the local stellar population. Another strategy is to correct for the extinction, which we adopt in this manuscript. The Gaia archive provides stellar extinctions that are based upon the General Stellar Parameterizer for Photometry (GSP-Phot) models. These GSP-Phot models use the BP and RP spectra to infer numerous stellar parameters, including extinction ([Andrae et al. 2023](#)). The extinction is quite small, The majority have  $A_{RP}$  and  $A_{BP} < 0.1$  and more than 90% are less than 0.2.

The Gaia DR3 catalog is incomplete in the galactic plane, especially for  $G < 3$ .<sup>1</sup> To ensure that we include all bright stars when inferring an age, this data set includes stars that appear in the Hipparcos catalog but are missing from Gaia DR3. To select all Hipparcos data within 150 pc, we use the same search cone as for the Gaia data: 1) Sky coordinates within 27 degrees of the Vela Pulsar position; 2) parallaxes between 2.2727 and 7.1429 mas. We convert the Johnson-Cousins magnitudes (V and I) to the Gaia bp and rp magnitudes ([Riello et al. 2021](#)); the color-color transformations give  $G_{BP} - V$  and  $G_{RP} - V$  as a function of third-order polynomials in  $V - I$ . After using the Hipparcos parallaxes to convert apparent magnitude to absolute magnitudes, we select all Hipparcos stars that are brighter than 0 in both BP and RP and that do not have a Gaia counterpart within 3 arcseconds. To identify the counterparts, we use the Gaia-Hipparcos cross correlations of [Brandt \(2021\)](#). This process adds 13 Hipparcos-only stars to the 705 stars in the Gaia sample, 6 of these are bright, evolved stars.

Figure 1 shows the absolute magnitudes of the selected stars with brightnesses brighter than 0 in both bands. The black dots represent the DR3 stars (705 stars) and the gold dots show the stars that appear only in the Hipparcos catalog (13 stars). The top panel shows the CMD for  $M_{RP}$  vs.  $M_{BP} - M_{RP}$ . The abscissa and ordinate of a CMD are correlated. To avoid modeling these correlations, *Stellar Ages* models the absolute magnitudes rather than modeling the CMD. The middle-right panel shows the absolute magnitudes of the same selected stars ( $M_{RP}$  vs.  $M_{BP}$ ). The middle-left and bottom-right panel

<sup>1</sup> See Section 14.3.1 and Figure 14.38 of the Gaia Data Release 3 documentation

shows the corresponding histograms. In their age inference, Kochanek (2022) included 9 stars that are in the Hipparcos catalog but not in DR3. Similarly, we find that there are 13 Hipparcos stars that are not included in Gaia DR3, 6 of which are bright, evolved stars. In the middle-right panel, the lower band of stars is the MS, and the upper band are red giants (RG) and red supergiants (RSG). Most of the RGs are old, low metallicity, halo stars. At the bright end, there are also bright giants and supergiants (Ib). However, there are no bright supergiants (Ia) (see section 5).

### 3. AGE-DATING THE STELLAR POPULATION USING SINGLE-STAR MODELS

To age-date the stellar population surrounding the Vela Pulsar, we use *Stellar Ages*, a code that uses magnitudes of individual stars to infer the distribution of ages, metallicities, and extinction for stellar populations. To infer this distribution, *Stellar Ages* uses the joint probability density function of magnitudes and a Gibbs Markov-chain Monte Carlo (MCMC) sampler. Specifically, *Stellar Ages* takes advantage of the fact that the joint probability density function of the magnitudes is known, representing the likelihood of observing a star within the color-magnitude diagram (CMD).

Most algorithms that infer ages or star formation histories infer the number of stars in a binned CMD (Dolphin 2002, 2012, 2013). The typical strategy is to discretize the CMD and model the likelihood of the number of stars within each color-magnitude bin. In particular, most algorithms use the Poisson distribution to calculate the likelihood of the observed number of stars in that bin. The full likelihood is then the joint probability of all bins. This strategy resembles the idea of using a Poisson process where the intensity is defined using the joint probability density function of the magnitudes. The main disadvantage of this strategy lies in the fact that the binning is arbitrary and leads to a loss of information. Additionally, the brightest bins have very few stars leading to large uncertainties. Since stars spend about 90% of their lives on the MS, most stars are MS stars. Hence, to avoid small-number statistics, one must include the bulk of the stars or MS stars. This strategy is effective for its designed purpose: inferring the star formation history for galaxies or entire regions of a galaxy. However, defining the likelihood in this way is not as effective in age-dating a few bright, evolved stars.

Rather than modeling the number of stars in the CMD, the novel algorithm *Stellar Ages* directly uses joint probability density functions to model the age for each star. This shift in statistical approach more effec-

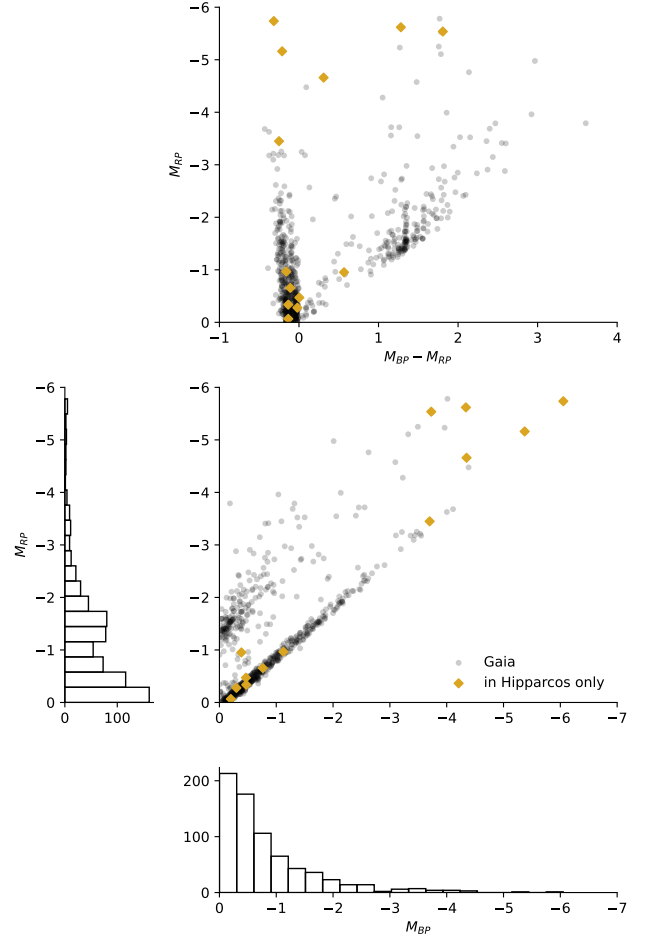


**Figure 1.** The absolute magnitudes of all stars within 150 pc of the Vela Pulsar. The top-right panel shows the color-magnitude diagram (CMD) for the Gaia red band,  $M_{RP}$ , vs. the Gaia colors,  $M_{BP} - M_{RP}$ . Rather than modeling the CMD, *Stellar Ages* models each individual magnitude; this avoids unnecessary correlations between the abscissa and the ordinate. The middle-right panel shows the absolute magnitudes for this stellar population. Both panels include all stars with apparent magnitudes  $\leq 0$  in both filters. While Gaia DR3 provides the largest collection of astrometric solutions at these distances, Gaia is unable to find solutions for the brightest stars. The full data set includes all stars from Gaia DR3 (black dots) and the missing stars that appear in the Hipparcos catalog only (golden dots).

tively maximizes the age information of a stellar population. For example, consider the following extremal case that highlights the benefit of inferring the age of each star. Consider the brightest, evolved star of a population. One could ask: how many stars do we expect in that region of the CMD for a given age? Even with the best-fitting age, the answer is  $1 \pm 1$ . This is a fairly large uncertainty, and it would take many more stars to reduce the uncertainty when using Poisson statistics.

However, we know that this one bright evolved star *exists*, so this is not really the relevant question. A more relevant question is: What is the likely age of that one observed star? For sufficiently bright stars, the answer can be quite restrictive. For example, a star with an absolute magnitude of -8.6 in F814W is 10 Myrs old or younger. This translates to a maximum mass that is at least  $19 M_{\odot}$ . It would only take a handful of the brightest stars from a 10 Myr old population to restrict the age to 10 Myrs with a high level of certainty. By changing the statistical question from “How many stars do we expect for a given age?” to “What is the likely age of each star?”, we maximize the information from the brightest stars.

In general, *Stellar Ages* infers the posterior distribution for age ( $t$ ), metallicity ( $[M/H]$ ), and the mean extinction,  $A_V$ . Because GSP-Phot already provides extinction corrections, we do not need to infer the mean extinction. Therefore, the model parameters are  $\theta = \{t, [M/H]\}$ . Schematically, the posterior distribution is:

$$P(\theta|D) \propto \mathcal{L}(D|\theta)P(t)P([M/H]). \quad (2)$$

The data ( $D$ ) are the set of magnitudes for all stars. The modeled magnitude in band ( $a$ ) of each star is

$$m_a = \tilde{m}_a(M, t, [M/H]) + A_a + e_a, \quad (3)$$

where  $\tilde{m}_a$  is the magnitude predicted by stellar evolution models as a function of  $t$ ,  $[M/H]$ , and the initial mass ( $M$ ) of the star (Bressan et al. 2012; Chen et al. 2014, 2015; Fu et al. 2018, PARSEC v1.2).  $e_a$  is a random error.  $A_a$  represents the extinction parameter in band  $a$ ; again GSP-Phot provides the extinction. In this analysis, we model two magnitudes, which are the Gaia absolute magnitudes BP and RP.

The joint likelihood of observing a star with magnitudes  $m_a$  and  $m_b$  is

$$\mathcal{L}(m_a, m_b|\theta) = \int p(m_a|\tilde{m}_a)p(m_b|\tilde{m}_b)p(\tilde{m}_a|\theta, M)p(\tilde{m}_b|\theta, M)p(M)dMd\tilde{m}_ad\tilde{m}_b. \quad (4)$$

This likelihood is the joint probability density function for a given age and metallicity.  $p(m_a|\tilde{m}_a)$  and  $p(m_b|\tilde{m}_b)$  are Gaussian distributions whose widths represent the observational uncertainties.  $p(\tilde{m}_a|\theta, M)$  and  $p(\tilde{m}_b|\theta, M)$  are delta functions and come directly from stellar evolution. Since  $\tilde{m}_a$  and  $\tilde{m}_b$  are not analytic, there is no closed analytic form for the joint probability density function. To approximate the likelihood, we note that the likelihood is the expectation of  $p(m_a|\tilde{m}_a)$  and  $p(m_b|\tilde{m}_b)$  with respect to the initial mass  $M$ . Therefore,

$$\begin{aligned} \mathcal{L}(m_a, m_b|\theta) &= E_M [p(m_a|\tilde{m}_a(\theta, M))p(m_b|\tilde{m}_b(\theta, M))] \\ &\approx \frac{1}{N_M} \sum_{\ell}^{N_M} p(m_A|\tilde{m}_A(\theta, M^{(\ell)}))p(m_B|\tilde{m}_B(\theta, M^{(\ell)})), \end{aligned} \quad (5)$$

where each  $M^{(\ell)}$  is a draw from  $P(M)$ , the initial mass function. To minimize sampling noise, we use perfect sampling instead of random sampling when drawing from this distribution.

Real stellar populations will likely be a mixture of populations with different ages and metallicities. Therefore, we propose a mixture data-generating model, or a weighted sum of the individual joint probability density functions:

$$\mathcal{L}(m_A, m_B|\{w_{t,z}\}_{t=1,z=1}^{T,Z}) = \sum_t^T \sum_z^Z w_{t,z} \mathcal{L}(m_A, m_B|\theta_{t,z}), \quad (6)$$

where  $w_{t,z}$  are weights for age index  $t$  and metallicity index  $z$ .

To infer the weights, we employ Bayesian statistics. Since sampling from the posterior distribution is not straightforward, we employ a Gibbs sampler algorithm that relies on the introduction of latent variables called labels ( $r_i$ ). These labels assign specific age, metallicity, and median extinction values to each star. Thus, the mixture model (6) is equivalently

$$\begin{aligned} (m_{A,i}, m_{B,i}|r_i = (t', z')) &\sim \mathcal{L}(m_A, m_B|\theta_{t',z'}) \\ r_i = (t', z')|\{w_{t,z}\}_{t=1,z=1}^{T,Z} &\sim w_{t',z'} \quad (i = 1 \dots N_{\text{stars}}). \end{aligned} \quad (7)$$

We complete the model specification by assigning a prior distribution to the weights. Specifically, we assume that

$$\{w_{t,z}\}_{t=1,z=1}^{T,Z} \sim \text{Dirichlet}(1, \dots, 1) \quad (8)$$

where  $\text{Dirichlet}(1, \dots, 1)$  denotes a  $(T \times Z)$ -dimensional Dirichlet distribution. Under model (7) with prior (8), the Gibbs sampler iterates between updating the labels and weights.

To update the labels, we sample from the conditional distribution

$$\begin{aligned} P(r_i = (t', z')|\{w_{t,z}\}_{t=1,z=1}^{T,Z}) \\ = \frac{w_{t',z'} p(m_{A,i}, m_{B,i}|\theta_{t',z'})}{\sum_t \sum_z w_{t,z} p(m_{A,i}, m_{B,i}|\theta_{t,z})} \quad (i = 1 \dots N_{\text{stars}}). \end{aligned} \quad (9)$$

To update the weights, we first compute the number of  $r_i$ ,  $i = 1 \dots N_{\text{stars}}$ , that are equal to  $(t', z')$  denoting the resulting count as  $N(t = t', z = z')$ . Then, we update the weights by sampling from the Dirichlet distribution:

$$\{w_{t,z}\}_{t=1,z=1}^{T,Z} | \{r_i\}_{i=1}^{N_{\text{stars}}} \\ \sim \text{Dirichlet}[1+N(t=1,z=1), \dots, 1+N(t=T,z=Z)]. \quad (10)$$

For more discussion on the techniques and validation tests of *Stellar Ages*, see Guzman et al. 2024.

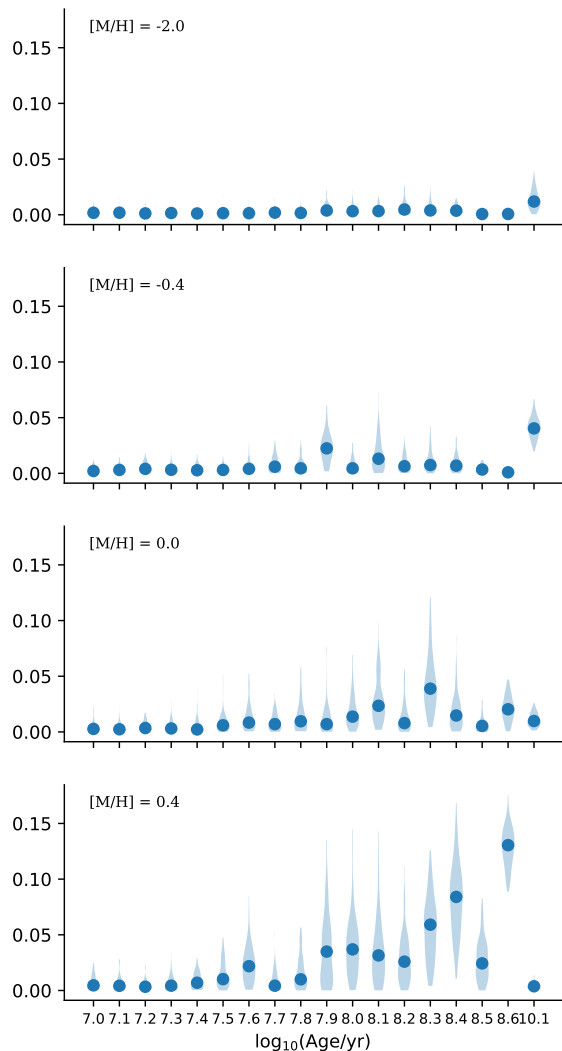
#### 4. THE STELLAR POPULATION IS INCONSISTENT WITH SINGLE-STAR EVOLUTION

Figure 2 presents the posterior distribution for the weights,  $w_{t,z}$ . Each panel presents violin plots as a function of log age,  $\log_{10}(t/\text{yr})$ , where each separate panel represents a different metallicity  $[M/H]$ . In this analysis, there are 1000 MCMC steps. We find that the solution converges within about 20 steps, so we burn the first 50 steps. MCMC draws tend to be correlated from one step to the next. To avoid this correlation and ensure that each MCMC draw is random, we select only every 10th step, resulting in 95 unique MCMC draws. The middle dot shows the median weight, and the width of the violin is proportional to the distribution of samples. Figure 3 also presents the weights but marginalized over  $[M/H]$ .

The weights for age (Fig. 3) indicate three general populations. One is old ( $\log_{10}(t/\text{yr}) = 10.1$ ) and low metallicity; these are halo stars in the vicinity of the Vela Pulsar. Most of the stars belong to a population that is greater than 80 Myrs old ( $\log_{10}(t/\text{yr}) \geq 7.9$ ). There is a hint of a population at 40 Myr ( $\log_{10}(t/\text{yr}) = 7.6$ ), but the weight for this population is significantly weaker than the other weights. Further analysis also shows that this age is actually inconsistent with the data.

In the process of inferring weights for stellar populations, *Stellar Ages* also infers the age for each star. Figure 4 plots  $M_{\text{RP}}$  vs.  $M_{\text{BP}}$ , and the color of the points indicates the most likely age. The G and K giants are clearly associated with the  $\log_{10}(t/\text{yr}) = 10.1$  population, and the vast majority of the MS stars are associated with the  $\geq 80$ -Myr-old population ( $\log_{10}(t/\text{yr}) \geq 7.9$ ). There are several bright blue and red stars which seem to be consistent with ages younger than 80 Myrs, however, the inference does not yield the corresponding MS stars. In fact, the brightest MS and giant stars are most consistent with younger ages ( $\log_{10}(t/\text{yr}) \leq 7.8$ ) and are not consistent with the bulk of the MS. Moreover, there is not a single stellar age that is consistent with these young-looking stars. Instead, they appear to be consistent with a wide range of young ages. These results are the first indication that the stellar population is inconsistent with single-star-evolution-only models.

Figure 5 compares the weighted model with the data. The brown dots show all stars with an older ( $\log_{10}(t/\text{yr}) > 7.8$ ) most likely age, and the white



**Figure 2.** Inferred ages and metallicities (weights) for the stellar population within 150 pc of the Vela Pulsar. The stellar isochrones included in this inference are the PARSEC single-star models. This violin plot summarizes the MCMC results for the weights. The central dot shows the median, and the "violin" shows the distribution of possible weights. Even though the brightest blue stars appear to be consistent with a young stellar population around  $\log_{10}(t/\text{yr}) = 7.6$ , the MCMC inference prefers a much older solution  $\log_{10}(t/\text{yr}) \geq 7.9$  or 8.0.

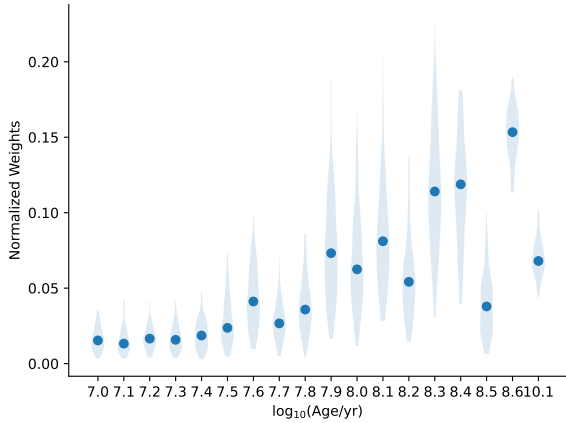


**Figure 3.** This figure shows the same inferred weights as in Fig. 2 but marginalized over metallicity ( $[M/H]$ ). *Stellar Ages* finds a possible young solution around  $\log_{10}(t/\text{yr}) = 7.6$  or 40 Myrs; however, the dominant weights are for ages  $\log_{10}(t/\text{yr}) \geq 7.9$  or  $\geq 80$  Myrs. Further inspection of the inference shows that the  $\log_{10}(t/\text{yr}) = 7.6$  solution is not only weak but also inconsistent with the data. See Figures 4-6.

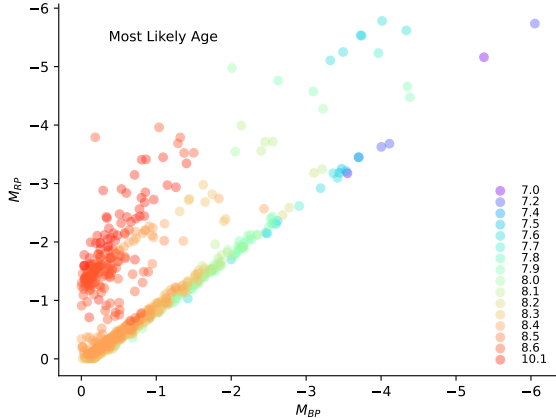


**Figure 4.** The most likely age for each star. In addition to inferring age weights for the entire population, *Stellar Ages* infers an age for each star. This enables an interrogation of which stars are contributing to which ages. For example, there are several bright, evolved stars that appear to be young ( $\log_{10}(t/\text{yr}) \leq 7.8$ ), but there are almost no MS stars with similar inferred ages. While not entirely apparent in this Figure, the number of red giants ( $M_{\text{RP}} \sim -3.5$  and  $M_{\text{BP}} \sim -2.5$ ) is far fewer than expected for the number of MS stars that are around 100 Myrs old (see Figure 6).

dots show the stars with a younger most likely age ( $\log_{10}(t/\text{yr}) \leq 7.8$ ). While the brightest evolved stars appear young in their brightness and colors, the best-fitting model assigns almost no MS stars to these young ages. Upon first glance, it appears that the weighted

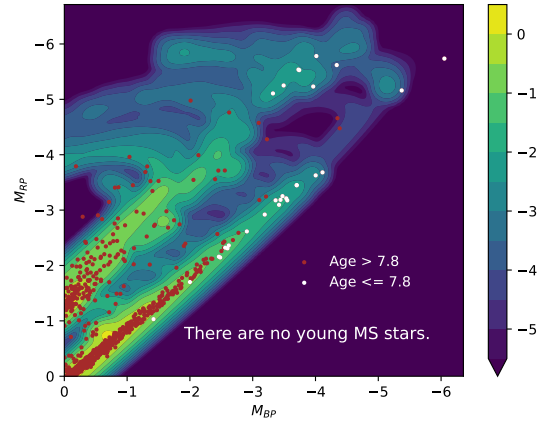


**Figure 5.** This figure compares the data with the weighted model. The brown dots represent all stars with older most likely ages ( $\log_{10}(t/\text{yr}) > 7.8$ ), while the white dots represent the stars with younger most likely ages ( $\log_{10}(t/\text{yr}) \leq 7.8$ ). While the brightest, evolved stars appear young, the best-fitting model has almost no MS stars with similar inferred ages. This is a major indication that the stellar population is inconsistent with a single-star-only.

model is consistent with the data. However, upon further inspection, the model predicts a higher relative number of stars in some areas and fewer number of stars in other areas.

Figure 6 most clearly illustrates this inconsistency. It shows the frequency distribution of the data and model as a function of  $M_{\text{RP}}$ . The solid blue histogram shows the distribution for the data that has an older most likely age ( $7.9 \leq \log_{10}(t/\text{yr}) \leq 8.3$ ), and the orange histogram corresponds to the data with the younger ( $\log_{10}(t/\text{yr}) \leq 7.8$ ) most likely age. For comparison, the blue, unfilled histogram shows the expected number of stars from the model (including weights with ages  $7.9 \leq \log_{10}(t/\text{yr}) \leq 8.3$ ). The model matches the MS distribution. However, the model predicts far more stars in the magnitude range  $-4.5 \gtrsim M_{\text{RP}} \lesssim -2.5$ . The model predicts 51.5 red giants in this magnitude range, but there are only 22. The Poisson probability of this is  $P(22|51.5) = 1.7 \times 10^{-6}$ . There is also a clear overabundance of young-looking stars. The data are clearly inconsistent with the best-fitting model, which suggests that the data are inconsistent with single-star models. The lack of red giants and the overabundance of young-looking blue evolved stars is consistent with recent binary evolution modeling (Menon et al. 2024). The most likely interpretation is that the bright blue and red stars are rejuvenated stars, which result from mergers and mass-gainers in binary evolution scenarios.

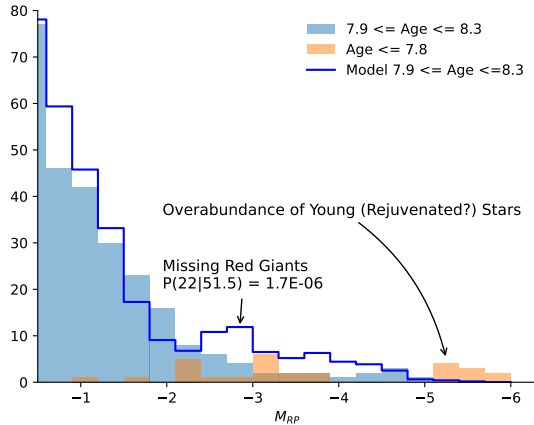


**Figure 6.** Distribution of stars as a function of the red Gaia absolute magnitude ( $M_{RP}$ ). The orange histogram shows the magnitudes for the young-looking stars ( $\log_{10}(t/\text{yr}) \leq 7.8$ ). The solid blue histogram shows the magnitude distribution for the stars that have ages of order 100 Myr old ( $7.9 \leq \log_{10}(t/\text{yr}) \leq 8.3$ ); the blue, unfilled histogram represents the corresponding expected number of stars from the weighted model. Given the number of observed MS stars, one would expect 51.5 red giants for this age. However, there are only 22. The Poisson probability of this result is  $1.7 \times 10^{-6}$ . At the same time, there is a clear overabundance of young-looking bright stars. These results are clearly inconsistent with the model that is based upon single-star evolution only. The most likely interpretation is that these young-looking, bright stars are rejuvenated stars (mergers or mass-gainers), resulting from binary evolution.

Thus far, all evidence indicates that the stellar population is inconsistent with single-star evolution only. There are two alternative hypotheses: 1) the brightest stars are run-away stars; 2) the brightest stars are either mass gainers or mergers. If 1) is true, then it would be possible that the progenitor of the Vela Pulsar was also a run-away star and its true age could be as young as the brightest stars imply. Gaia offers a way to test this scenario. If there is a large population of young run-away stars, then the young-looking stars should have relatively high space velocities compared to the other stars. Figure 7 shows the transverse proper motion (top panel), transverse space velocities (middle panel), and velocity dispersion (lower panel) for all stars within 150 pc of the Vela Pulsar and that have  $M_{BP}$  and  $M_{RP} < 0$ . As expected from dynamical relaxation, the velocity dispersion increases with age. More to the point, all of the young-looking stars have relatively low space velocities compared to the local stars. We conclude that the space velocities of the young-looking stars is inconsistent with the run-away star scenario. Rather,

the young-looking stars are most likely mass gainers or the product of mergers.

## 5. SIMBAD CROSSMATCHING: THE BRIGHTEST, BLUE AND RED STARS SHOW SIGNIFICANT EVIDENCE OF BINARY EVOLUTION

The conclusions of this paper hinge upon the odd brightness and color distributions of the brightest stars. Therefore an important question is: are the BP and RP absolute magnitudes correct, or is there some systematic error with the brightest stars? The GSP-Phot extinctions are predominantly small, but those inferences rely on low-resolution spectra and single-star models. Could GSP-Phot inferences be systematically incorrect? Also, the Hipparcos stars have no extinction information; given the low extinction values from GSP-Phot, we just assumed zero extinction for the Hipparcos stars. Is it possible that some of the bright giants (luminosity class II) and supergiants (Ib) are actually bright supergiants (Ia)? Is it possible that some of the giants are actually bright MS stars? It is unlikely that a large number of stars have systematic errors large enough to account for the discrepancies that we observe; the correction for 10s of bright giants would need to be of order 2 magnitudes. While it might be unlikely that 10s of stars have errors this large, it is important to validate spectral and brightness classifications of the brightest stars.

To verify the absolute magnitudes, we cross match the brightest, blue and red stars with objects in the SIMBAD Database. First, we crossmatch all stars with absolute magnitudes brighter than  $M_{RP} = -3.5$ . We crossmatch the Gaia sources and SIMBAD sources based upon a 2 arcsecond circle in sky coordinates. Within this set, there are many bright giants (luminosity class III) and supergiants (Ib), and almost no bright supergiants (Ia). In general, the Gaia magnitudes and colors are consistent with the published luminosity and spectral types. This confirms that, as the GSP-Phot inferences show, the extinctions do not affect the magnitudes much at all.

In addition, we crossmatch the 28 young-looking, bright stars with objects in SIMBAD; this crossmatch is quite illuminating in that a large majority of these stars show strong indications of binary evolution. Table 1 lists the resulting crossmatched stars.

There are three peculiar bright, blue evolved stars.  $\zeta$  Puppis is an evolved O supergiant with strong winds and rotation. The other two objects are multiple star systems.  $\gamma^2$  Vel (Regor) is a spectroscopic binary composed of a Wolf-Rayet star and a blue giant. In fact,  $\gamma^2$  Vel is actually part of the quadruple star system  $\gamma$  Vel.  $\epsilon$  Car B is a binary system consisting of a K giant and

**Table 1.** Stellar properties of the young-looking stars with inferred ages  $\log_{10}(t/\text{yr}) \leq 7.8$ . The Name, Object type (Object), and Spectral Type (Sp Type) are properties reported by the SIMBAD database after crossmatching. The spectral types confirm the GSP-Phot inferences, which further supports the extinction estimates.  $\zeta$  Puppis is an evolved O supergiant with strong winds and rotation.  $\gamma^2$  Vel (Regor) is a spectroscopic binary composed of a Wolf-Rayet star and a blue giant.  $\epsilon$  Car B is a binary system consisting of a K giant and a B MS star. 8 of the young-looking stars on the MS are Be stars; as a class, Be stars show evidence for rapid rotation, which is a natural consequence of binary evolution. 3 of the stars are either spectroscopic binaries (SB) or eclipsing binaries (EclBin). Hence, a sizeable fraction of the young-looking stars show evidence for recent binary evolution.  $G_{BP}$  and  $G_{RP}$  are the Gaia absolute magnitudes after correcting for the parallax, zero point, and extinction.

Gaia Young-looking Stars					
Name	Object	Sp Type	Gaia ID	BP	RP
* kap CMa	Be*	B1.5Ve	5583216215017531648	-4.11	-3.68
* sig CMa	RedSG	K5Ib	5610441600394646016	-4.01	-5.78
* r Pup	Be*	B1V	5544672044638408832	-4.00	-3.63
* ksi Pup	Star	G6Ib	5614471482318442240	-3.96	-5.23
* c Pup	Star	K4III	5538814190283894656	-3.74	-5.53
* E Car	Be*	B3III	5222191159719547776	-3.70	-3.45
* P Pup	**	B0III	5530670107652889344	-3.55	-3.18
* p Car	Be*	B4Vne	5253796346624992128	-3.53	-3.21
* h01 Pup	RedSG	K4.5Ib	5540591825707339648	-3.49	-5.25
V* V Pup	EclBin	B1Vp+B2:	5517171678276669696	-3.47	-3.25
* alf Pyx	Variable*	B1.5III	5639188675501966464	-3.44	-3.18
* ups01 Pup	Be*	B2V+B3IVne	5589411172768195840	-3.42	-3.10
* ome CMa	Be*	B2.5Ve	5610257226031514240	-3.36	-3.18
* t02 Car	Star	K4/5(III)	5350588691660896128	-3.32	-5.11
HD 69081	Be*	B2(V)	5541637564345383808	-3.19	-2.92
* L Vel	Star	B2IV	5312887640522116992	-2.91	-2.62
HD 66194	Be*	B3Vn	5290767631226220032	-2.62	-2.36
V* IS Vel	bCepV*	B2V	5516167755443050368	-2.60	-2.31
* b Pup	SB*	B2V	5537733610870346880	-2.56	-2.32
HD 64740	Star	B2V	5517239366958299776	-2.48	-2.14
V* QS Pup	bCepV*	B2III	5530577267638216832	-2.46	-2.16
HD 79275	PulsV*	B2III/IV	5327525954211395968	-2.00	-1.70
HD 62560A	Star		5535394155060356480	-1.42	-1.03
Hipparcos Young-looking Stars					
Name	Object	Sp Type	HIP ID	BP	RP
* zet Pup	BYDraV*	O4I(n)fp	39429	-6.05	-5.74
* gam02 Vel	WolfRayet*	WC8+O7.5III-V	39953	-5.37	-5.16
* eps Car B	Star	B2Vp	41037	-4.34	-5.62
* eps Car	**	K3:III+B2:V	44816	-3.73	-5.54
* eps Car A	Star	K3:III	45941	-3.70	-3.45

a B MS star. Furthermore, 8 of the young-looking stars are Be stars. As a class, Be stars show strong signs of rapid rotation; for example, the emission lines are often attributed to an excretion disk surrounding the star that results from the star rotating near break up speeds, high resolution interferometric observations show disk-like or oblate shapes, and high Doppler broadening indicates rapid rotation (Porter & Rivinius 2003). Such rapid rotation could be a natural consequence of binary evolution (Pols et al. 1991; Portegies Zwart 1995; Shao &

Li 2014; Staritsin 2022). 3 of the stars are either confirmed spectroscopic binaries (SB) or eclipsing binaries (EclBin). Hence, at least half of the young-looking stars show strong signs of binary evolution.

## 6. DISCUSSION AND CONCLUSIONS

The primary conclusion is that the brightness and color distribution of the stellar population within 150 pc of the Vela Pulsar are inconsistent with single-star evolution models only. Evidence for the inconsistency is as follows. A *Stellar Ages* inference suggests that

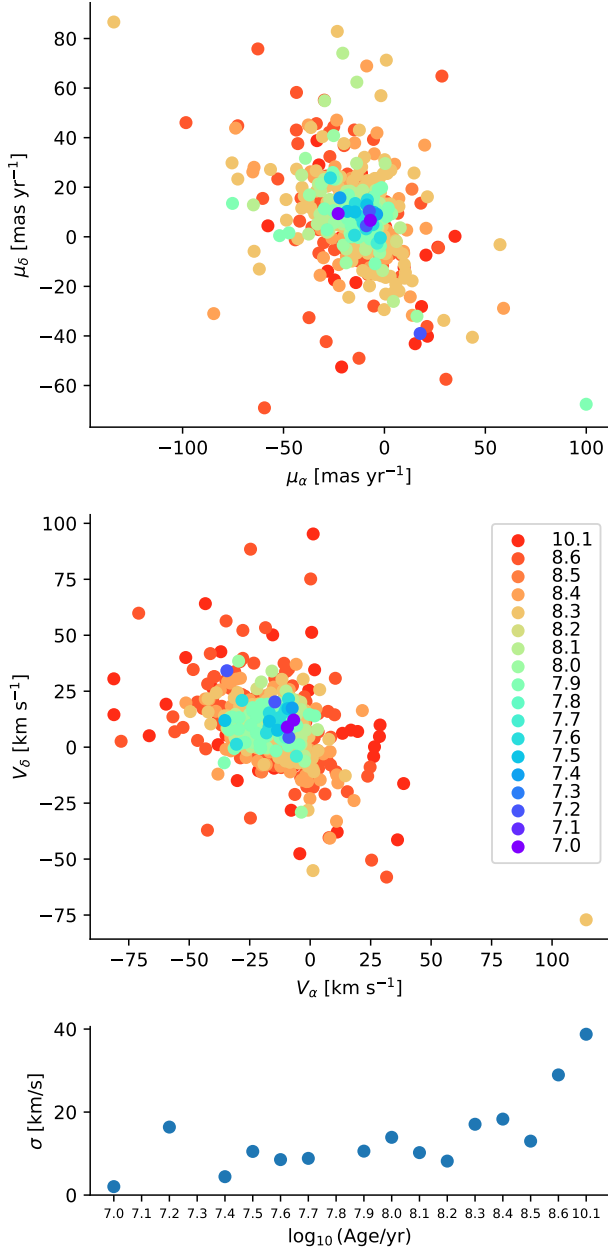


**Figure 7.** The transverse proper motions (top panel), space velocities (middle panel), and velocity dispersion (bottom panel) for all stars with  $M_{\text{RP}}$  and  $M_{\text{BP}} < 0$  within 150 pc of the Vela Pulsar. The color indicates the inferred ages of each individual star. There are two hypotheses that could explain the odd distribution of the bright MS and giant stars. One is that the brightest stars are mass gainers and/or mergers. The second hypothesis is that these odd stars are run-away stars and associated with neighboring stellar populations. However, the brightest, young-looking stars have relatively low transverse space velocities. Therefore, the brightest stars are unlikely run-away stars; it is more likely that they are mass gainers and/or mergers.

the youngest, dominant population is  $\geq 80$  Myrs old. Given the number of MS stars with this age, there is a lack of associated red giants. There are 22, when the model expects 51.5; the Poisson probability of this result is  $P(22|51.5) = 1.7 \times 10^{-6}$ . While there is a lack of red giants associated with a  $\geq 80$ -Myr-old population, there is an overabundance of stars that appear much younger (10-40 Myrs old). Yet, the best-fitting single-star model does not indicate a corresponding young MS. Crossmatching the young-looking stars with the SIMBAD catalog indicates that at least half of the young-looking stars are the result of binary evolution. Furthermore, a lack of red giants and an overabundance of blue supergiants is consistent with the effects of binary evolution (Menon et al. 2024). Hence, the stellar population surrounding the Vela Pulsar is inconsistent with single-star evolution only, and the most likely scenario is that the young-looking stars are rejuvenated stars (mergers or mass-gainers).

Given these observations, we inductively reason that the Vela Pulsar progenitor was  $\geq 80$  Myr old when it exploded and that it was a mass gainer or a merger. If true, then this is the first clear association of an older stellar population and a CCSN. The conclusion that the Vela Pulsar progenitor was a merger is not surprising. In fact, observations of massive stars indicate a large binary fraction with small separations, which in turn suggests a large number of mergers. Binary evolution theory in fact predicts that of order 10% of CCSNe have binary mergers as their progenitors. What is surprising is that this is the first clear association with an older population.

Kochanek (2022) also inferred the age of the Vela Pulsar stellar population and also found a young age (25 to 30 Myr) for the youngest stellar population. However, that analysis modeled collective numbers in the color-magnitude diagram (CMD), whereas the analysis of this manuscript models the age of each individual star as well. It is this higher statistical fidelity that makes it clear that the young age is inconsistent with the stellar population and likely a result of assuming single-star models only in the fits.

The conclusions of this manuscript lead to some clear predictions that must be tested further. For one, binary evolution suggests that merger products should be rapidly rotating. Are all of the young-looking stars rapidly rotating? Secondly, this manuscript demonstrates the inconsistency of using single-star models only to model the stellar brightness and colors. Would models that include binary evolution be more consistent with the stellar population surrounding the Vela Pulsar?

## ACKNOWLEDGMENTS

JWM was supported by the Los Alamos National Laboratory (LANL) through its Center for Space and Earth Science (CSES). CSES is funded by LANL's Laboratory Directed Research and Development (LDRD) program under project number 20210528CR. This work was supported by NASA through grant HST-GO-16778.017-A from the Space Telescope Science Institute, which is operated by the Association of Universities for Re-

search in Astronomy, Inc., under NASA contract NAS 5-26555. This work has made use of data from the European Space Agency (ESA) mission *Gaia* (<https://www.cosmos.esa.int/gaia>), processed by the *Gaia* Data Processing and Analysis Consortium (DPAC, <https://www.cosmos.esa.int/web/gaia/dpac/consortium>). Funding for the DPAC has been provided by national institutions, in particular the institutions participating in the *Gaia* Multilateral Agreement.

## REFERENCES

- Andrae, R., Fouesneau, M., Sordo, R., et al. 2023, *A&A*, 674, A27, doi: [10.1051/0004-6361/202243462](https://doi.org/10.1051/0004-6361/202243462)
- Aschenbach, B., Egger, R., & Trümper, J. 1995, *Nature*, 373, 587, doi: [10.1038/373587a0](https://doi.org/10.1038/373587a0)
- Badenes, C., Harris, J., Zaritsky, D., & Prieto, J. L. 2009, *ApJ*, 700, 727, doi: [10.1088/0004-637X/700/1/727](https://doi.org/10.1088/0004-637X/700/1/727)
- Barker, B. L., O'Connor, E. P., & Couch, S. M. 2023, *ApJL*, 944, L2, doi: [10.3847/2041-8213/acb052](https://doi.org/10.3847/2041-8213/acb052)
- Bartunov, O. S., Blinnikov, S. I., Pavlyuk, N. N., & Tsvetkov, D. Y. 1994, *A&A*, 281, L53
- Brandt, T. D. 2021, *ApJS*, 254, 42, doi: [10.3847/1538-4365/abf93c](https://doi.org/10.3847/1538-4365/abf93c)
- Bressan, A., Marigo, P., Girardi, L., et al. 2012, *MNRAS*, 427, 127, doi: [10.1111/j.1365-2966.2012.21948.x](https://doi.org/10.1111/j.1365-2966.2012.21948.x)
- Bruenn, S. W., Lentz, E. J., Hix, W. R., et al. 2016, *ApJ*, 818, 123, doi: [10.3847/0004-637X/818/2/123](https://doi.org/10.3847/0004-637X/818/2/123)
- Burrows, A., & Goshy, J. 1993, *ApJL*, 416, L75, doi: [10.1086/187074](https://doi.org/10.1086/187074)
- Burrows, A., & Vartanyan, D. 2021, *Nature*, 589, 29, doi: [10.1038/s41586-020-03059-w](https://doi.org/10.1038/s41586-020-03059-w)
- Chen, Y., Bressan, A., Girardi, L., et al. 2015, *MNRAS*, 452, 1068, doi: [10.1093/mnras/stv1281](https://doi.org/10.1093/mnras/stv1281)
- Chen, Y., Girardi, L., Bressan, A., et al. 2014, *MNRAS*, 444, 2525, doi: [10.1093/mnras/stu1605](https://doi.org/10.1093/mnras/stu1605)
- Couch, S. M., Warren, M. L., & O'Connor, E. P. 2020, *ApJ*, 890, 127, doi: [10.3847/1538-4357/ab609e](https://doi.org/10.3847/1538-4357/ab609e)
- Díaz-Rodríguez, M., Murphy, J. W., Rubin, D. A., et al. 2018, *ApJ*, 861, 92, doi: [10.3847/1538-4357/aac6e1](https://doi.org/10.3847/1538-4357/aac6e1)
- Díaz-Rodríguez, M., Murphy, J. W., Williams, B. F., Dalcanton, J. J., & Dolphin, A. E. 2021, *MNRAS*, 506, 781, doi: [10.1093/mnras/stab1800](https://doi.org/10.1093/mnras/stab1800)
- Dodson, R., Legge, D., Reynolds, J. E., & McCulloch, P. M. 2003, *ApJ*, 596, 1137, doi: [10.1086/378089](https://doi.org/10.1086/378089)
- Dolphin, A. E. 2002, *MNRAS*, 332, 91, doi: [10.1046/j.1365-8711.2002.05271.x](https://doi.org/10.1046/j.1365-8711.2002.05271.x)
- . 2012, *ApJ*, 751, 60, doi: [10.1088/0004-637X/751/1/60](https://doi.org/10.1088/0004-637X/751/1/60)
- . 2013, *ApJ*, 775, 76, doi: [10.1088/0004-637X/775/1/76](https://doi.org/10.1088/0004-637X/775/1/76)
- Fu, X., Bressan, A., Marigo, P., et al. 2018, *MNRAS*, 476, 496, doi: [10.1093/mnras/sty235](https://doi.org/10.1093/mnras/sty235)
- Gaia Collaboration, Prusti, T., de Bruijne, J. H. J., et al. 2016, *A&A*, 595, A1, doi: [10.1051/0004-6361/201629272](https://doi.org/10.1051/0004-6361/201629272)
- Gaia Collaboration, Vallenari, A., Brown, A. G. A., et al. 2022, arXiv e-prints, arXiv:2208.00211. <https://arxiv.org/abs/2208.00211>
- Ghosh, S., Wolfe, N., & Fröhlich, C. 2021, arXiv e-prints, arXiv:2107.13016. <https://arxiv.org/abs/2107.13016>
- Gogarten, S. M., Dalcanton, J. J., Murphy, J. W., et al. 2009, *ApJ*, 703, 300, doi: [10.1088/0004-637X/703/1/300](https://doi.org/10.1088/0004-637X/703/1/300)
- Gogilashvili, M., & Murphy, J. W. 2022, *MNRAS*, 515, 1610, doi: [10.1093/mnras/stac1811](https://doi.org/10.1093/mnras/stac1811)
- Hansen, B. M. S., & Phinney, E. S. 1997, *MNRAS*, 291, 569
- Hillier, D. J., & Dessart, L. 2012, *MNRAS*, 424, 252, doi: [10.1111/j.1365-2966.2012.21192.x](https://doi.org/10.1111/j.1365-2966.2012.21192.x)
- Jennings, Z. G., Williams, B. F., Murphy, J. W., et al. 2014, *ApJ*, 795, 170, doi: [10.1088/0004-637X/795/2/170](https://doi.org/10.1088/0004-637X/795/2/170)
- Kasen, D., & Woosley, S. E. 2009, *ApJ*, 703, 2205, doi: [10.1088/0004-637X/703/2/2205](https://doi.org/10.1088/0004-637X/703/2/2205)
- Kochanek, C. S. 2022, *MNRAS*, 511, 3428, doi: [10.1093/mnras/stac098](https://doi.org/10.1093/mnras/stac098)
- Koplitz, B., Johnson, J., Williams, B. F., et al. 2021, *ApJ*, 916, 58, doi: [10.3847/1538-4357/abfb7b](https://doi.org/10.3847/1538-4357/abfb7b)
- . 2023, *ApJ*, 949, 32, doi: [10.3847/1538-4357/acc249](https://doi.org/10.3847/1538-4357/acc249)
- Large, M. I., Vaughan, A. E., & Mills, B. Y. 1968, *Nature*, 220, 340, doi: [10.1038/220340a0](https://doi.org/10.1038/220340a0)
- Lentz, E. J., Bruenn, S. W., Hix, W. R., et al. 2015, *ApJ*, 807, L31, doi: [10.1088/2041-8205/807/2/L31](https://doi.org/10.1088/2041-8205/807/2/L31)
- Lindegren, L., Bastian, U., Biermann, M., et al. 2021, *A&A*, 649, A4, doi: [10.1051/0004-6361/202039653](https://doi.org/10.1051/0004-6361/202039653)
- Mabanta, Q. A., Murphy, J. W., & Dolence, J. C. 2019, *ApJ*, 887, 43, doi: [10.3847/1538-4357/ab4bcc](https://doi.org/10.3847/1538-4357/ab4bcc)
- Menon, A., Ercolino, A., Urbaneja, M. A., et al. 2024, *ApJL*, 963, L42, doi: [10.3847/2041-8213/ad2074](https://doi.org/10.3847/2041-8213/ad2074)
- Moriya, T., Tominaga, N., Blinnikov, S. I., Baklanov, P. V., & Sorokina, E. I. 2011, *MNRAS*, 415, 199, doi: [10.1111/j.1365-2966.2011.18689.x](https://doi.org/10.1111/j.1365-2966.2011.18689.x)

- Morozova, V., Piro, A. L., Renzo, M., et al. 2015, *ApJ*, 814, 63, doi: [10.1088/0004-637X/814/1/63](https://doi.org/10.1088/0004-637X/814/1/63)
- Müller, B. 2015, *MNRAS*, 453, 287, doi: [10.1093/mnras/stv1611](https://doi.org/10.1093/mnras/stv1611)
- . 2016, *Publications of the Astronomical Society of Australia*, 33, e048, doi: [10.1017/pasa.2016.40](https://doi.org/10.1017/pasa.2016.40)
- Murphy, J. W., & Dolence, J. C. 2017, *ApJ*, 834, 183, doi: [10.3847/1538-4357/834/2/183](https://doi.org/10.3847/1538-4357/834/2/183)
- Pejcha, O., & Thompson, T. A. 2012, *ApJ*, 746, 106, doi: [10.1088/0004-637X/746/1/106](https://doi.org/10.1088/0004-637X/746/1/106)
- Pols, O. R., Cote, J., Waters, L. B. F. M., & Heise, J. 1991, *A&A*, 241, 419
- Portegies Zwart, S. F. 1995, *A&A*, 296, 691
- Porter, J. M., & Rivinius, T. 2003, *PASP*, 115, 1153, doi: [10.1086/378307](https://doi.org/10.1086/378307)
- Riello, M., De Angeli, F., Evans, D. W., et al. 2021, *A&A*, 649, A3, doi: [10.1051/0004-6361/202039587](https://doi.org/10.1051/0004-6361/202039587)
- Sana, H., de Mink, S. E., de Koter, A., et al. 2012, *Science*, 337, 444, doi: [10.1126/science.1223344](https://doi.org/10.1126/science.1223344)
- Shao, Y., & Li, X.-D. 2014, *ApJ*, 796, 37, doi: [10.1088/0004-637X/796/1/37](https://doi.org/10.1088/0004-637X/796/1/37)
- Smartt, S. J. 2015, *PASA*, 32, e016, doi: [10.1017/pasa.2015.17](https://doi.org/10.1017/pasa.2015.17)
- Staritsin, E. 2022, *Research in Astronomy and Astrophysics*, 22, 105015, doi: [10.1088/1674-4527/ac8f8d](https://doi.org/10.1088/1674-4527/ac8f8d)
- Strotjohann, N. L., Ofek, E. O., Gal-Yam, A., et al. 2023, arXiv e-prints, arXiv:2303.00010, doi: [10.48550/arXiv.2303.00010](https://doi.org/10.48550/arXiv.2303.00010)
- Sukhbold, T., Ertl, T., Woosley, S. E., Brown, J. M., & Janka, H.-T. 2016, *ApJ*, 821, 38, doi: [10.3847/0004-637X/821/1/38](https://doi.org/10.3847/0004-637X/821/1/38)
- Van Dyk, S. D. 2017, *Philosophical Transactions of the Royal Society of London Series A*, 375, 20160277, doi: [10.1098/rsta.2016.0277](https://doi.org/10.1098/rsta.2016.0277)
- Vartanyan, D., Burrows, A., Radice, D., Skinner, M. A., & Dolence, J. 2018, *MNRAS*, 477, 3091, doi: [10.1093/mnras/sty809](https://doi.org/10.1093/mnras/sty809)
- Williams, B. F., Hillis, T. J., Murphy, J. W., et al. 2018, ArXiv e-prints. <https://arxiv.org/abs/1803.08112>
- Woosley, S. E., Heger, A., & Weaver, T. A. 2002, *Reviews of Modern Physics*, 74, 1015, doi: [10.1103/RevModPhys.74.1015](https://doi.org/10.1103/RevModPhys.74.1015)
- Zapartas, E., de Mink, S. E., Izzard, R. G., et al. 2017, *A&A*, 601, A29, doi: [10.1051/0004-6361/201629685](https://doi.org/10.1051/0004-6361/201629685)